

# **Lattice Boltzmann Method for Single Phase Heat Transfer and Two Phase Drop & Bubble Dynamics**

**National Institute of Technology, Rourkela  
(Deemed University)**

In partial fulfillment of the requirement for the degree of

**Master of Technology**

in

**Mechanical Engineering  
(Thermal Engineering Specialization)**

by

**Sandeep Shreshth  
(Roll No. 211ME3186)**

Under the guidance of  
**Dr. Suman Ghosh**



**Department of Mechanical Engineering  
National Institute of Technology  
Rourkela -769 008 (India)  
June, 2013**





**National Institute of Technology  
Rourkela**

## **CERTIFICATE**

This is to certify that the report entitled "LATTICE BOLTZMANN METHOD FOR SINGLE PHASE HEAT TRANSFER AND TWO PHASE DROP & BUBBLE DYNAMICS" submitted to the National Institute of Technology, Rourkela by Sandeep Shreshth Roll No. 211ME3186 for the award of the Degree of Master of Technology in Department of Mechanical Engineering with specialization in Thermal Engineering is a record of bona fide work carried out by him under our supervision and guidance.

Place: NIT Rourkela, Rourkela-769008, Orissa.

Date: June 3, 2013

**Dr. Suman Ghosh**

Assistant Professor

Department of Mechanical Engineering  
NIT Rourkela, Rourkela-769008, India



# ACKNOWLEDGEMENT

I express my deep sense of gratitude towards my thesis supervisor **Dr. Suman Ghosh** for providing their unwavering support, encouragement and consummate feedback throughout the course of this study and in the participation of this thesis. Without his illustrious guidance this thesis would not have seen the light of the day.

After the completion of this Thesis, I experience the feeling of achievement and satisfaction. Looking into the past I realize how impossible it was for me to succeed on my own. I wish to express my deep gratitude to all those who extended their helping hands towards me in various ways during my short tenure at NIT Rourkela.

I express my sincere thanks to **Professor K.P. MAITY, HOD, Department of Mechanical Engineering**, and also the other staff members of Department of Mechanical Engineering, NIT Rourkela for providing me the necessary facilities that is required to conduct the experiment and complete my thesis.

Special thanks to **Dr. Arup Kumar Das**. He provided me unflinching encouragement and support in various ways. His truly scientist intuition has made him as a constant oasis of ideas and passions in research, which exceptionally inspire and enrich my growth as a student want to be.

I need to further thank all my friends, and special thanks to Shahnawaz Ahmed who always took the time to listen, even when I was just complaining.

Last but not the least I am especially indebted to my parents for their love, sacrifice, and support. They are my first teachers after I came to this world and have set great examples for me about how to live, study, and work.

**Date: June 03, 2013**

**SANDEEP SHRESHTH**



# Contents

<b>Description</b>	<b>Page no</b>
<b>Title</b>	<b>i</b>
<b>Certificate</b>	<b>iii</b>
<b>Acknowledgement</b>	<b>v</b>
<b>Contents</b>	<b>vii</b>
<b>List of Symbols</b>	<b>ix</b>
<b>List of Figures</b>	<b>xi</b>
<b>Abstract</b>	<b>xiii</b>
<b>Chapter 1: Introduction and Literature Review</b>	<b>1</b>
1.1 Introduction	2
1.2 Literature Review	6
1.3 Gaps in the literature	9
1.4 Aims and Objective	10
1.5 Organization of the Thesis	10
<b>Chapter 2: Lattice Boltzmann Formulation</b>	<b>13</b>
2.1 2D diffused interface based LBM	14
2.2 3D diffused interface based LBM	19
<b>Chapter 3: Problem Statement</b>	<b>21</b>
3.1 Single phase heat transfer in 2D square domain	22
3.2 Effect of fluid velocity on dynamics of drop	23
3.3 Effect of cross-section on bubble shape formation	24
3.4 Dynamics of bubble and drop through inclined channel	25
<b>Chapter 4: Results and Discussion</b>	<b>27</b>
4.1 Single phase heat transfer in 2D square domain	28
4.1.1 High temperature at bottom plane	28

4.1.2 High temperature at top and bottom plane	30
4.2 Effect of fluid velocity on dynamics of drop	30
4.3 Effect of cross-section on bubble shape	32
4.4 Dynamics of bubble and drop through inclined channel	34
4.4.1 Effect of channel inclination on bubble	34
4.4.2 Effect of bubble volume	35
4.4.3 Effect of channel inclination on drop	37
4.4.4 Effect of drop volume	39
<b>Chapter 5: Conclusion and Future Scope</b>	<b>41</b>
5.1 Concluding Remarks	42
5.2 Scope of the Future Work	43
<b>References</b>	<b>45</b>

# List of Symbols

$n$	total number density
$\phi$	density difference (phase order parameter)
$u$	macroscopic velocity of the fluid
$\theta_M$	mobility
$F_b$	body force
$P$	pressure tensor
$\mu_\phi$	chemical potential
$c_i$	velocity vector of lbm
$f_i$	distribution function
$g_i$	distribution function
$\rho_H$	high density of the fluid
$\rho_L$	low density of the fluid
$\tau_\phi$	relaxation parameter
$t$	time
$A$	amplitude parameter
$k$	curvature of the interface
$\sigma$	surface tension
$W$	diffused interface width
$\Gamma$	mobility coefficient



# LIST OF FIGURES

Figure No.	Description	Page No.
Figure 2.1	Computational 3D domain for a single rising bubble: (a) Initial position (b) Final position	14
Figure 2.2	D2Q9 lattice structure used for 2D model	15
Figure 2.3	D3Q19 lattice structure used for 3D model	19
Figure 3.1	Single phase heat transfer in 2D square domain	22
Figure 3.2	Effect of fluid velocity on dynamics of drop	23
Figure 3.3	Effect of channel cross-section on bubble	24
Figure 3.4	Effect of channel inclination ( $60^{\circ}$ inclination with horizontal) (a) on bubble (b) on drop	25
Figure 4.1	Temperature contour of 2D Square domain with $100^{\circ}$ c at bottom plane	28
Figure 4.2	Temperature profile of vertical mid plane for 2D square domain with $100^{\circ}$ c at bottom plane	29
Figure 4.3	Temperature contour of 2D square domain for top and bottom plane at $100^{\circ}$ c and remaining at $0^{\circ}$ c.	29
Figure 4.4	Temperature profile for vertical mid plane for temperature of $100^{\circ}$ c at top and bottom plane	30
Figure 4.5	Effect of liquid velocity ( $V_L$ ) on the dynamics of drop: (a) $V_L = 0\text{m/s}$ (b) $V_L = 0.1\text{m/s}$ (c) $V_L = 0.2\text{m/s}$ (d) $V_L = 0.3\text{m/s}$	31
Figure 4.6	Effect of channel size on bubble shape at different time step	32
Figure 4.7	Deformed bubble at particular time step	33
Figure 4.8	Effect of channel cross-section on the bubble shape	33
Figure 4.9	Effect of channel size on velocity of bubble	34
Figure 4.10	Effect of channel inclination on bubble asymmetry for (a) $90^{\circ}$ inclination (b) $60^{\circ}$ inclination and (c) $30^{\circ}$ inclination.	35

Figure 4.11	Effect of bubble volume on the shape of bubble in vertical channel with (a) volume = $4.08 \times 10^{-4} \text{ m}^3$ (b) volume = $2.68 \times 10^{-4} \text{ m}^3$ (c) volume = $1.79 \times 10^{-4} \text{ m}^3$	36
Figure 4.12	Effect of bubble volume on the shape of bubble in $60^\circ$ inclined channel with (a) volume = $4.08 \times 10^{-4} \text{ m}^3$ (b) volume = $2.68 \times 10^{-4} \text{ m}^3$ (c) volume = $1.79 \times 10^{-4} \text{ m}^3$	37
Figure 4.13	Effect of bubble volume on the shape of bubble in $30^\circ$ inclined channel with (a) volume = $4.08 \times 10^{-4} \text{ m}^3$ (b) volume = $2.68 \times 10^{-4} \text{ m}^3$ (c) volume = $1.79 \times 10^{-4} \text{ m}^3$	37
Figure 4.14	Effect of channel inclination on drop asymmetry for (a) $90^\circ$ inclination (b) $60^\circ$ inclination (c) $30^\circ$ inclination.	38
Figure 4.15	Effect of drop volume on the shape of drop in vertical channel with (a) volume = $4.08 \times 10^{-4} \text{ m}^3$ (b) volume = $2.68 \times 10^{-4} \text{ m}^3$ (c) volume = $1.79 \times 10^{-4} \text{ m}^3$	39
Figure 4.16	Effect of drop volume on the shape of drop in $60^\circ$ inclined channel with (a) volume = $4.077 \times 10^{-4} \text{ m}^3$ (b) volume = $2.6808 \times 10^{-4} \text{ m}^3$ (c) volume = $1.795 \times 10^{-4} \text{ m}^3$	40
Figure 4.17	Effect of drop volume on the shape of drop in $30^\circ$ inclined channel with (a) volume = $4.077 \times 10^{-4} \text{ m}^3$ (b) volume = $2.6808 \times 10^{-4} \text{ m}^3$ (c) volume = $1.795 \times$	40

# Abstract

A Lattice Boltzmann Method (LBM) has been adopted for modelling and simulation of single phase heat transfer and multiphase flow dynamics. At first the energy equation in a test problem involving thermal conduction has been solved and then an investigation has been made about the suitability of scalar diffusion in LBM for a new class of problems. This is a 2D steady state single phase conduction heat transfer problem with Dirichlet boundary conditions. Parametric study has been made by varying different boundary conditions and temperature contours are plotted. Then the hydrodynamics of water drop in a moving liquid is studied. Velocity of the liquid flowing in the channel is varied to establish the effect of medium velocity on final shape and motion of the drop. Diffuse interface concept is adopted to track the interfacial dynamics. Thirdly, the hydrodynamics of a bubble in a stationary medium in a rectangular channel have been investigated by varying the size of the channel. At last, numerical simulation of an air bubble and water drop in an inclined rectangular is also studied. The effects of channel inclination, and bubble size on the shape of the bubble have also been studied.

**Keywords:** Bubble and drop dynamics, lattice Boltzmann, inclined channel, Two phase flow



# **Chapter 1**

**Introduction**

**and**

**Literature survey**

## **1.1 Introduction**

The lattice Boltzmann method (LBM) has received much attention in science and engineering as a potential computational technique for solving a large class of problems. Among many other types of problems, the LBM has been successfully used to simulate a wide range of fluid flow and heat transfer problems. Lattice Boltzmann method is widely used to solve the various heat transfer problems involving thermal conduction, convection and radiation because of its potential application in engineering designs and energy related problems such as solar collectors, cooling of electronic component, thermal insulation, heat exchangers etc. and in various fluid flows such as flow over porous media, flow through various pipe fittings such as return bends, sudden contraction or enlargement etc. Attempt has been made to solve energy equation in a test problem involving thermal conduction and then an investigation has been made about the suitability of scalar diffusion in LBM for a new class of problems. The LBM is emerging as a versatile computational method that has many advantages. In comparison to the conventional CFD solvers like the finite difference method, the finite element method and the finite volume method, the advantages of the LBM comprises of a clear physical meaning, a simple calculation procedure, simple and more efficient implementation for parallel computation, straightforward and efficient handling of complex geometries and boundary conditions, high computational performance with regard to stability and precision.

Fluid motion can take a variety of forms ranging from simple flows such as laminar flow in a pipe, to more complex flows such as vortex shedding behind cylinders, wave motion and turbulence. It incorporates both liquid and gaseous flows. Many of the different flow situations are multiphase flow. Attention has been given on two phase/multiphase flow as they are often encountered in nature as well as in

different industrial processes. Applications of multiphase flows are plenty like combustion, chemical reactions, boiling, petroleum refining and in other heat and mass transfer processes. With the implication of engineering knowledge in daily life problems, multiphase flow is becoming more relevant for different attractive fields like filling the fuel tank of a Formula 1 racing car within few seconds, oil jet splashing within the cylinders of racing engines, etc.

The simplest configuration of multiphase flow is the rise of gaseous/air bubble due to buoyancy inside a liquid column. The dynamics of bubble moving in a fluid medium has crucial ramifications in research, industrial processing and natural processes. Due to its wide application, bubble dynamics in liquid column has been studied by number of researchers both experimentally and theoretically. In the experimental investigations, researchers are continuously making efforts to predict the Taylor bubble shape and velocity in a stationary or moving liquid column. Though the shape of the interface is simple in such phenomena, it has been studied by many researchers due to its immense application in various processes ([Bhaga and Weber 1981](#); [Bozanno and Dente 2001](#)). Steady shape of the bubble and its terminal velocity depends on the resistive drag force as well as the buoyancy force on a rising bubble. To model the shape and dynamics of the interface knowledge of surface tension force is of utmost important. Configuration of the interface and the force due to surface tension are interrelated to each other. The treatment of these two factors is difficult for multiphase flows specially when there exist a large density ratio between the fluids.

Numerical simulations have been adapted to study the interfacial dynamics of the bubble in liquid media. In conventional CFD models of two phase flow, a set of Navier-Stokes equations are solved and the interface is captured by using volume of

fluid (VOF) or level set methods. But interface reconstruction using VOF becomes complicated for three dimensional cases whereas level set method violates mass conservation for its application in large topological changes. Recently, the lattice Boltzmann method (LBM) has been developed into an alternative and promising numerical scheme for simulating multicomponent fluid flows. The LBM has great advantages over conventional methods for multiphase flows. It does not only track interfaces, but can maintain sharp interfaces without any artificial treatments. Also, the LBM is accurate for the mass conservation of each component fluid. Although lattice Boltzmann method (LBM) has emerged as an alternate and promising tool for simulation of complex two-phase flow problems as compared to the conventional CFD solver for Navier-Stokes equation. It takes care about the features of the micro-scale or meso-scale as well as conserves the macroscopic variables. LBM can handle multiphase systems and complex interfaces with ease and efficiency. Lattice Boltzmann technique seems to be most robust and showed fair predictability in different thermo-physical problems. A brief description of basic lattice Boltzmann methodology is presented next which shows the flexibility of the method in solution of the complex hydrodynamics.

The lattice Boltzmann method is a powerful technique for the computational modeling of a wide variety of complex fluid flow problems including single and multiphase flow in complex geometries. It is a discrete computational method based upon the Boltzmann equation. It considers a typical volume element of fluid to be composed of a collection of particles that are represented by a particle velocity distribution function for each fluid component at each grid point. The LBM is a derivative of the lattice gas automata (LGA) method which was first proposed about a dozen years ago by a number of physicists. LGA method was first proposed by [Friseh](#)

et al. in 1986. The motivation behind the development of such a model originated from the fact that with its inherent microscopic origin, the model is expected to have a broader range of applications than the macroscopic Navier Stokes equations. The microscopic simulation can essentially provide more detailed information that is important to reveal the underlying physics behind complex fluid behavior. Although a direct solution of the full Boltzmann transport equation will provide necessary microscopic details, it would be a rather cumbersome task, due to high possible dimensions of the distribution functions. As a compromising alternative, it has been assumed that the movements of fluid particles are restricted only in few assigned directions. This leads to the concept of discrete velocity methods based on the lattice structures. LBM has been derived from the generalized LGA model by effectively representing space and time discretized version of the conservation equations in the form of the Boltzmann transport equations. The main aim behind the description of macroscopic phenomena within the viewpoint of lattice structure is to describe the physical nature of fluids from a more statistical orientation. This provides more feasible hydrodynamic solutions as compared to that in the macroscopic viewpoint. In recent years, the Lattice Boltzmann Method (LBM) has emerged as a promising numerical method for simulating fluid flows. Unlike conventional methods which solve the discretized macroscopic Navier-Stokes equations, the LBM is based on microscopic particle models and mesoscopic kinetic equations. The fundamental concept of the LBM is to construct simplified kinetic models that incorporate the essential physics of microscopic or mesoscopic processes so that the macroscopic averaged properties obey the desired macroscopic equations. The LBM is especially useful for modeling interfacial dynamics, flows over porous media, and multi-phase flows. In addition, the LBM algorithm tends to be very simple, allowing parallelism in

a straightforward manner. Nowadays, the method has quickly found its way in dealing with a number of engineering flow problems. However, the underlying lattice gas (or mesh) is a rectangle (or a hexagon) in two dimensions or a cube (or a shape with perfect geometric symmetry) in three dimensions, equivalent to the regular Cartesian grid used by conventional Navier-Stokes solvers. As a result, solution domains with inclined or curved boundaries are approximated by staircase-like steps. This restriction severely limits the applicability of LBM as most of the industrial and practical flows have complex flow geometries. Looking back on the history of the conventional Navier-Stokes methods, the issue of mesh flexibility dominates its development. It begins with the Cartesian regular grid, then the use of body-fitted coordinate grids and structured multi-block grids, and finally the widespread acceptance of unstructured grids, allowing the greatest flexibility in adapting the grid to domain boundaries. The body-fitted method and the multi-block structured method are merely special cases of the more general unstructured mesh. This method naturally accommodates a variety of boundary conditions such as the pressure drop across the interface between two fluids and wetting effects at a fluid-solid interface. It is an approach that bridges microscopic phenomena with the continuum macroscopic equations. Further, it can model the time evolution of systems.

## **1.2 Literature survey**

Gaseous bubble in liquid column is commonly encountered in variety of industrial applications such as oil refineries, nuclear reactors etc. Due to its wide applications, substantial literature can be found to reveal the underlying physics either by experimental observation or theoretical evolution. Bubble dynamics in liquid column is studied by number of researchers by both experimental ([Tung and Parlange, 1976](#); [Kataoka et al, 1987](#); [Polonsky et al, 1999](#)) and theoretical ([Tudose and Kawaji, 1999](#);)

investigation. Starting from initial experimental investigation of [Zukoski \(1966\)](#) to recent effort of [Lu and Prosperetti \(2009\)](#) researchers are continuously making effort to predict the simplest Taylor drop shape and velocity in a stationary or moving liquid column. Continuous efforts have been done to predict the Taylor bubble shape and velocity under the flow of surrounding fluid or quiescent fluid. Most of the studies related to Taylor bubble are confined in the gas-liquid domain. On the other hand, a denser fluid, if placed on top of a lighter fluid, causes downward movement in the form of a Taylor drop. The shape of the Taylor drop is more or less equivalent to the shape of a Taylor bubble.

To the best of the knowledge of the authors, very few efforts have been made to study the gas-liquid Taylor bubble and liquid-liquid Taylor drop inside an inclined column. Complexities increase further when the conduit through which the bubble or the drop is traversing gets more inclination. The bubble/drop takes an asymmetric shape across the conduit axis which largely affects its dynamics. In industry, pipe fittings are essential component of any two-phase flow system. Thus two-phase invariably contain a variety of pipe fittings which may involve a change in channel area such as sudden contraction or sudden enlargement in flow direction. The flow of two-phase mixtures across sudden expansions and contractions is relevant in many applications such as chemical reactors, power generation units, oil wells and petrochemical plants. As the two-phase mixture flows through the sudden area changes, the flow might form a separation region at the sharp corner. Continuous efforts are also still going on to equip LBM for tackling complex interfacial dynamics. [Rothman and Keller \(1988\)](#) first proposed color method and gave a concept to transition across the interface or diffused interface. Diffused layer can be identified by the non-zero gradient of the color field assigned differentially to different fluids.

[Shan et al. \(1993\)](#) introduced a new potential method which can identify the interfacial layer by the potential gradient similar to the color method. But Potential method also fails to describe the evolution of the interface. Later on, [Swift et al. \(1995\)](#) proposed free energy method which defines a distribution function and its conservation equation throughout the domain. [He et al. \(1999\)](#) came with a new idea of correlating fluid mobility with their respective density field. A new lattice Boltzmann scheme has been proposed for simulation of multi-phase flow in the nearly incompressible limit. The numerical stability is improved by reducing the effect of numerical errors in calculation of molecular interactions. An index function is used to track interfaces between different phases. Numerical simulations were carried out for the two-dimensional Rayleigh–Taylor in-stability developed from both single-mode and multiple-mode initial perturbations. The evolution of the conservation equation takes a form of convection diffusion equation and turns out to be modified Cahn–Hilliard equation after suitable approximation.

[Takada et al. \(2000\)](#) have described the numerical simulation results of bubble motion under gravity by the lattice Boltzmann method (LBM), which assumes that a fluid consists of mesoscopic fluid particles repeating collision and translation and a multiphase interface are reproduced in a self-organizing way by repulsive interaction between different kinds of particles. The two-dimensional results by LBM agree with those by the Volume of Fluid method based on the Navier-Stokes equations. Obtained results prove that the buoyancy terms and the 3D model proposed here are suitable, and that LBM is useful for the numerical analysis of bubble motion under gravity.

[Inamuro et al. \(2004\)](#) have proposed a lattice Boltzmann method for two-phase immiscible fluids with large density differences. The difficulty in the treatment of large density difference is resolved by using the projection method. The method can

be applied to simulate two-phase fluid flows with the density ratio up to 1000. To show the validity of the method, they have applied the method to the simulations of capillary waves, binary droplet collisions, and bubble flows.

Zheng et al. (2006) described the lattice Boltzmann model for simulating multiphase flows with large density ratios. The method is easily implemented. The interface capturing equation is recovered without any additional terms as compared to other methods. The method is further verified by its application to capillary wave and the bubble rising under buoyancy with comparison to other method.

Mandal et al. (2008) have worked on an experimental study on the shape and stability of liquid Taylor bubbles and liquid Taylor drops in vertical and inclined tubes. The effect of tube inclination, tube diameter, and pipe material on shape, stability, and velocity of a liquid Taylor bubbles and liquid Taylor drops has been explained qualitatively from basic physics. It is observed that the shape of the nose in vertical tubes is spherical. Ripples are observed at the tail region of a Taylor bubble and drop.

### **1.3 Gaps in literatures**

The above discussion gives a broad overview of the multitude research activities carried out so far on the analysis of multiphase flows heat transfer problems. From the literature survey one can make out the aspects where further research is necessary.

Some of the gaps in literature are as follows:

1. Very few efforts have been made to solve energy equation for single phase heat transfer problems using LBM.
2. Established CFD techniques are not suitable for tracking complex interface for multi-phase flow.

3. However the recently developed Lattice Boltzmann method overcomes all limitations and can be used to model the multiphase flow successfully.
4. Two phase flow inside an inclined channel of rectangular cross-section is a challenging task to solve numerically. Very few efforts have been made in this direction.

## **1.4 Aims and Objectives**

From the literature survey conclusion can be drawn that very few efforts have been done to investigate the suitability for simulation of single phase heat transfer problems using LBM. The capturing of non-linear hydrodynamics of the bubble or drop moving in surrounding medium inside vertical and inclined channel has not been studied in details. On the other hand, due to numerical difficulties, asymmetric bubble or drop movement in an inclined channel has not been investigated in details. Based on the lacuna of the literature following objectives are identified for the present work:

1. Effort has to be made to solve energy equation and then to investigate the suitability of scalar diffusion in LBM for new class of problems.
2. Effect of primary phase velocity on the movement of drop inside the vertical channel will be modeled using LBM.
3. Effect of channel size on the shape of bubble will be modeled numerically.
4. To capture the asymmetry in the shape of the bubble or drop under different inclinations of the channel, numerical model will be developed.

## **1.5 Organization of the Thesis**

The thesis is organized into five different chapters. First Chapter contains introduction of multiphase flow and various heat transfer phenomena. Preliminary concepts along with brief review of earlier works of the dynamics of bubble and drop have been

discussed. Brief history of evolution of lattice Boltzmann method has been described. Based on the review of earlier works gaps in literatures and scope of present work have been described. Second chapter deals with the basic methodology used for modeling the dynamics of bubbles or drop is described. Third chapter contains problem description in detail. Four different problems have been studied. Fourth chapter deals with results and discussion of the problem described in third chapter. Fifth chapter deals with concluding remarks based on the results obtained in chapter 4. Potential future areas of research are also identified in this chapter.



# **Chapter 2**

## **Lattice Boltzmann Formulation**

In this chapter the 2D lattice Boltzmann model proposed by Zheng et al. (2006) has been described in detail. Based on this 2D model, 3D version of diffused interface based formulation has been developed. A rectangular parallelepiped section of  $L_x \times L_y \times L_z$  dimension has been taken as the problem domain. To see the bubble dynamics initially a spherical bubble is placed at the bottom of the domain filled with liquid (Figure 2.1.a). Due to its own dynamics bubble will take a bullet shape as has been shown in Figure 2.1.b. Further simulation is done for bubble movement when velocity provided in liquid and for simulation of inclined channel the domain has been inclined with a prescribed angle.

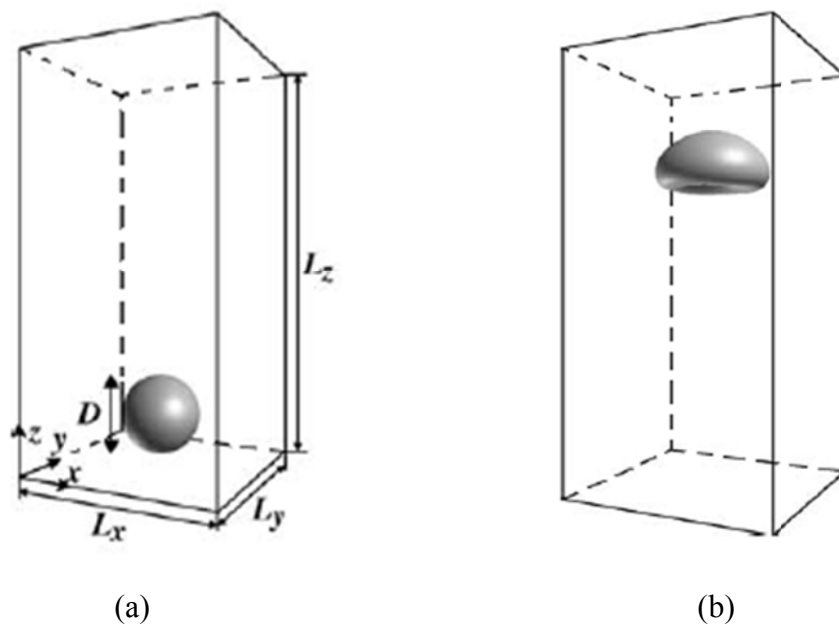


Figure 2.1: Computational 3D domains for a single rising bubble: (a) Initial position (b) Final position. (Inamuro et al. 2004)

## 2.1 2D Diffused interface based LBM

A basic model to track the two-phase flow is developed based on lattice Boltzmann methodology. Diffused interface concept is considered to track the interfacial behavior. As domain is associated with two different fluids and their mutual interactions two derived properties have been defined based on the respective

densities  $\rho_L$  and  $\rho_H$ . The properties and their corresponding definitions are described as:

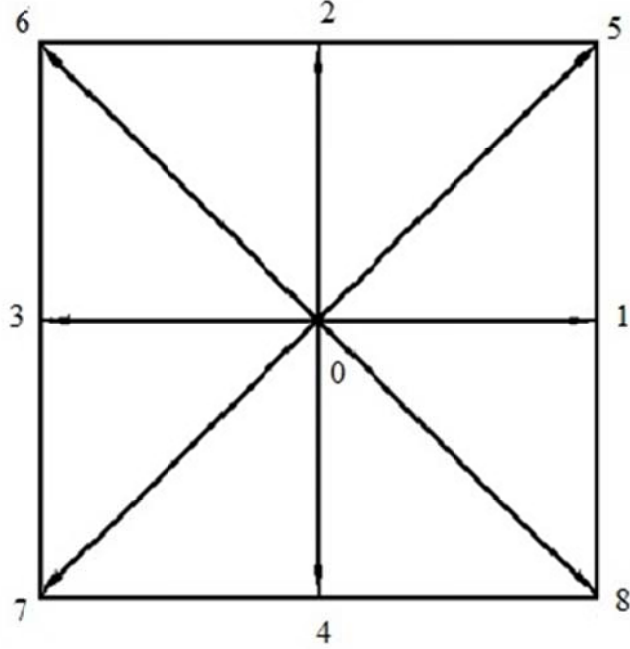


Figure 2.2: D2Q9 lattice structure used for 2D model

$$\Phi = \frac{\rho_H - \rho_L}{2} \quad \text{and} \quad n = \frac{\rho_H + \rho_L}{2} \quad (2.1)$$

The dynamics of the two fluids inside the domain follows conservation equations and an interface capturing equation which can be written as:

$$\frac{\partial n}{\partial t} + \nabla \cdot (n\bar{u}) = 0 \quad (2.2)$$

$$\frac{\partial (n\bar{u})}{\partial t} + \nabla \cdot (n\bar{u}\bar{u}) = -\nabla \cdot \mathbf{P} + \mu \nabla^2 \bar{u} + F_b \quad (2.3)$$

$$\frac{\partial \Phi}{\partial t} + \nabla \cdot (\Phi\bar{u}) = \theta_m \nabla^2 \mu_\Phi \quad (2.4)$$

Where,  $\mathbf{P}$  is the pressure tensor,  $\mu_\Phi$  is the chemical potential,  $\theta_m$  is the mobility,  $F_b$  is

the body force associated with the flow.

A statistical description of a fluid system can be made in terms of a distribution function  $f_i(\bar{x},t)$  in the basis of lattice Boltzmann equation. D2Q9 lattice structure as has been shown in Figure 1.1, has been used for the propagation of information of  $f_i(\bar{x},t)$ . Using LBM approximation equation (2.2-2.3) can be written as:

$$f_i(\bar{x} + \bar{c} \delta t, t + \delta t) = f_i(\bar{x}, t) + \frac{f_i^{eq}(\bar{x}, t) - f_i(\bar{x}, t)}{\tau_n} + \left(1 - \frac{1}{2\tau_n}\right) \frac{w_i}{c_s^2} \left[ (\bar{c} - \bar{u}) + \frac{\bar{c} \cdot \bar{u}}{c_s^2} \bar{c} \right] (\mu_\Phi \nabla \Phi + F_b) \delta t \quad (2.5)$$

Where,

$$f_i^{eq} = w_i A_i + w_i n \left( 3c_{i\alpha} u_\alpha - \frac{3}{2} u^2 + \frac{9}{2} u_\alpha u_\beta c_{i\alpha} c_{i\beta} \right) \quad (2.6)$$

With coefficients as:

$$A_1 = \frac{9}{4} n - \frac{15(\Phi \mu_\Phi + n/3)}{4}$$

$$A_i = 3(\Phi \mu_\Phi + n/3) \quad (2.7)$$

$$w_0 = \frac{4}{9}, w_{i=1,2,3,4} = \frac{1}{9}, w_{i=5,6,7,8} = \frac{1}{36}$$

In Eq. (2.5)  $\tau_n$  is the relaxation parameter which can be directly related with viscosity of the fluid. To accommodate the diffused interface concept in Eq. (2.5) Zheng et al (2006) defined chemical potential  $\mu_\Phi$  as follows:

$$\mu_\Phi = A(4\Phi^3 - (\rho_H - \rho_L)^2 \Phi) - k \nabla^2 \Phi \quad (2.8)$$

Here, A is amplitude parameter used to control the interaction of energy between two phases and k is the curvature of the interface. These two parameters are related with surface tension,  $\sigma$  and diffused interface width, W as:

$$W = \frac{2\sqrt{k/A}}{\rho_H - \rho_L} \quad \text{and} \quad \sigma = \frac{4\sqrt{k/A}}{3} (\rho_H - \rho_L)^3 \quad (2.9)$$

To capture the dynamics of the interface modified Cahn-Hilliard equation is simulated.

Order Parameter  $g_i(\bar{x},t)$  has been assigned to replicate the interface dynamics. The

conservation equation of, can be written using LBM approximation:

$$g_i(\bar{x} + \bar{e}_i \delta t, t + \delta t) - g_i(\bar{x}, t) = (1-q) [ g_i(\bar{x} + \bar{e}_i \delta t, t + \delta t) - g_i(\bar{x}, t) ] + \frac{g_i^{eq}(\bar{x}, t) - g_i(\bar{x}, t)}{\tau_\phi} \quad (2.10)$$

Here,  $\tau_\phi$  is a dimensionless relaxation time,  $\bar{e}_i$  is lattice velocity and  $q$  is constant coefficient.

Equilibrium distribution of  $g_i(\bar{x}, t)$  can be written as:

$$g_i^{eq} = A_i + B_i \Phi + C_i \Phi \bar{c} \cdot \bar{u} \quad (2.11)$$

Where, the coefficients are taken as,

$$\begin{aligned} A_i &= -2\Gamma\mu_\phi \\ B_1 &= 1, B_i = 0 \\ C_i &= \frac{1}{2q} \end{aligned} \quad (2.12)$$

$\Gamma$  is used to control the mobility and is defined as,

$$\theta_M = q \left( \tau_\phi q - \frac{1}{2} \right) \delta(\Gamma) \quad (2.13)$$

Where  $q$  is implicit parameter. The relation between  $q$  and  $\tau_\phi$  is as follows:

$$q = \frac{1}{\tau_\phi + 0.5} \quad (2.14)$$

The macroscopic parameter  $\Phi$  is evaluated from equilibrium distribution function  $g_i(\bar{x}, t)$  as:

$$\Phi = \sum_i g_i \quad (2.15)$$

As the phenomena are surface tension related it can be related as:

$$F_s = -\nabla \cdot P = -\Phi \nabla \mu_\Phi - \nabla p_o \quad (2.16)$$

Where  $p_o = n c_s^2$ ,  $c_s$  being the speed of sound. Modified Navier-Stokes equation

after incorporation of diffused interface concept can be written as:

$$\frac{\partial n}{\partial t} + \nabla \cdot (n \bar{u}) = 0 \quad (2.17)$$

$$\frac{\partial (n \bar{u})}{\partial t} + \nabla \cdot (n \bar{u} \bar{u}) = -\Phi \nabla \mu_\Phi - \nabla p_o + \mu_\Phi \nabla \Phi + \mu \nabla^2 \bar{u} + F_b \quad (2.18)$$

The pressure tensor is calculated as:

$$P = A (3 \Phi^4 - 2 \Phi^{*2} \Phi^2 - \Phi^{*4}) - k \Phi \nabla^2 \Phi + \frac{(\nabla \Phi)^2}{2} + \frac{n}{3} \quad (2.19)$$

Where A is amplitude parameter used to control the interaction of energy between two phases.

$$\Phi = \Phi^* \tanh(2\zeta/W) \quad (2.20)$$

$\zeta$  is the coordinate which is perpendicular to the interface and W is the thickness of the interface layer.

Here, the expected order parameter is:

$$\Phi^* = \frac{\rho_H - \rho_L}{2} \quad (2.21)$$

From equations (2.8) and (2.20) we can obtain:

$$\mu_\Phi \nabla_\zeta \Phi = \frac{3\sigma}{W^2} \tanh^3(2\zeta/W) \text{sech}^2(2\zeta/W) \quad (2.22)$$

Thus the potential form of surface tension related term is independent of the density and density difference. It is obvious from equation (2.22) that  $\mu_\Phi \nabla_\zeta \Phi$  is related with the surface tension coefficient and the width of interface layer.

## 2.2 3D Diffused interface based LBM

The domain is discretized using 3D cubic lattice to replicate the inclined channel. The physical information is propagated using D3Q19 structure of the lattice, is shown in Figure 2.3.

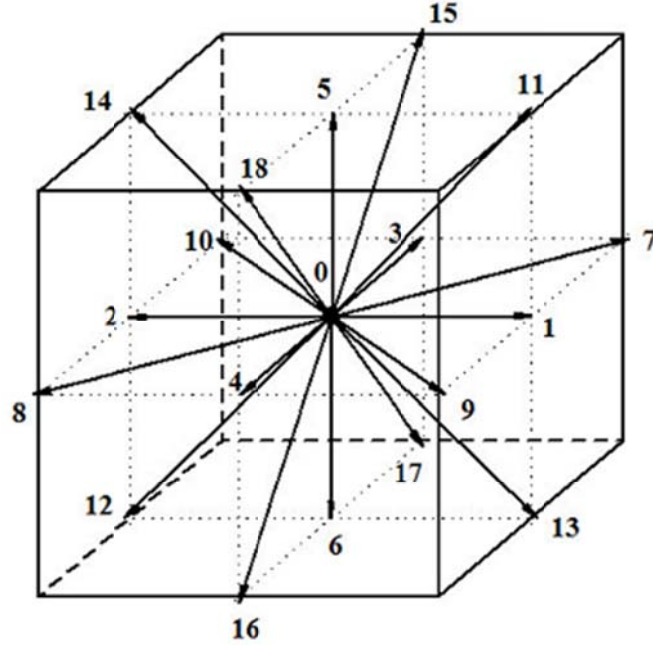


Figure 2.3: D3Q19 lattice structure used for 3D model

This model is similar kind of the 2D model described above but due to more number of lattice direction involved, directional velocities and weight parameters are adapted accordingly. Directional velocities can be written as:

$$e_i = \begin{cases} (0,0,0) & i = 1 \\ (\pm 1, 0, 0), (0, \pm 1, 0), (0, 0, \pm 1) & i = 2, 3, \dots, 7 \\ (\pm 1, \pm 1, 0), (\pm 1, 0, \pm 1), (0, \pm 1, \pm 1) & i = 8, 9, \dots, 19 \end{cases} \quad (2.23)$$

Weight parameter for 19 different directions can be written as:

$$w_0 = \frac{1}{3}, w_{i=1,2,3,\dots,6} = \frac{1}{18}, w_{i=7,8,9,\dots,18} = \frac{1}{36} \quad (2.24)$$

The macroscopic properties like density and velocity of the domain can be calculated from,  $f_i(\bar{x},t)$  and  $g_i(\bar{x},t)$  as:

$$n = \sum_{i=1,..,19} ( f_i (\bar{x}, t) ) \quad (2.25)$$

$$u = [(\sum_{i=1,..,19} ( f_i (\bar{x}, t) ) \bar{e}_i ) + \frac{1}{2} (\mu_\Phi \nabla \Phi + F_b)] / n \quad (2.26)$$

$$\Phi = \sum_{i=1,..,19} ( g_i (\bar{x}, t) ) \quad (2.27)$$

# **Chapter 3**

## **Problem Statement**

In this chapter problems have been described in detail based on gaps in literatures cited in Chapter 1. Four problems have been studied which is described in details below:

### 3.1 Single phase heat transfer in 2D square domain

In the present problem single phase heat conduction through a 2D square domain has been studied using Lattice Boltzmann Method. Dirichlet boundary condition is provided in square domain and temperature contours have been plotted. A lattice Boltzmann Method (LBM) is used to solve the energy equation in a test problem involving thermal conduction and to thus investigate the suitability of scalar diffusion in LBM for a new class of problems.

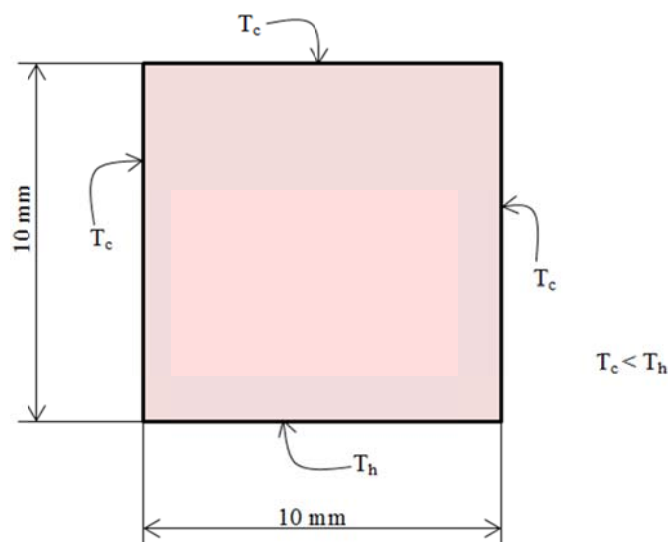


Figure 3.1: Single phase heat transfer in 2D square domain

The problem is chosen as steady state single phase conductive heat transfer in a 2-D square enclosure of 10 mm  $\times$  10 mm with dirichlet boundary conditions as shown in Figure 3.1. A parametric variation is done with different temperature boundary conditions and temperature contours and graphs are plotted.

### 3.2 Effect of fluid velocity on dynamics of drop

Here, the effect of velocity of surrounding fluid on the dynamics of the drop is studied. 2D methodology as proposed in Chapter 2 has been used for the simulation. The dynamics of a liquid drop in the surrounding of a lighter liquid has been modeled using the described methodology. The schematic representation of the problem is shown in Figure 3.2.



Figure 3.2: Effect of fluid velocity on dynamics of drop

Water has been taken as drop liquid and channel has been considered to be filled with kerosene. For the numerical simulation of dynamics of drop density of water has been taken as  $1000 \text{ kg/m}^3$  and that of kerosene is  $787 \text{ kg/m}^3$ . The diameter of the drop is taken as  $30 \text{ mm}$  and the channel dimension has been considered as  $120 \text{ mm} \times 500 \text{ mm}$ . To replicate the no slip boundary condition at the solid vertical wall bounce back condition is applied for the lattices adjacent to it. Constant inlet velocity has been provided at top boundary to simulate dynamics of drop under the different flow situations. Periodic

boundary condition is maintained at the inlet and outlet of the tube to avoid end effect. Two lattice unit interfacial widths have been allowed to model the complex liquid-liquid interactions.

### 3.3 Effect of cross-section on bubble shape formation

In this case the effect of conduit configurations on the shape of the bubble is studied. Three different conduit configurations (110 mm × 500 mm, 130 mm × 500 mm and 150 mm × 500 mm) have been chosen for simulation. Periodic boundary condition is maintained at the inlet and outlet of the channel to avoid end effect. No slip boundary condition at the solid vertical wall is applied. Bubble is placed in the water column symmetrically as shown in Figure 3.3. The volume of bubble is kept constant ( $5.236 \times 10^{-4} \text{ m}^3$ ) and establish the effect of conduit configuration. Density of bubble and water medium are taken as  $1 \text{ kg/m}^3$  and  $1000 \text{ kg/m}^3$  respectively.

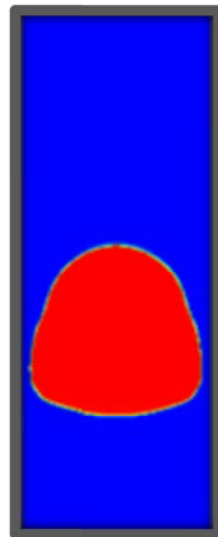


Figure 3.3: Effect of channel cross-section on bubble

### 3.4 Dynamics of bubble and drop through inclined channel

In this chapter dynamics of bubble and liquid drop through a liquid filled inclined channel has been studied. In this case a developed 3D lattice Boltzmann model has been used for simulation of dynamics of bubble and drop through the inclined channel.

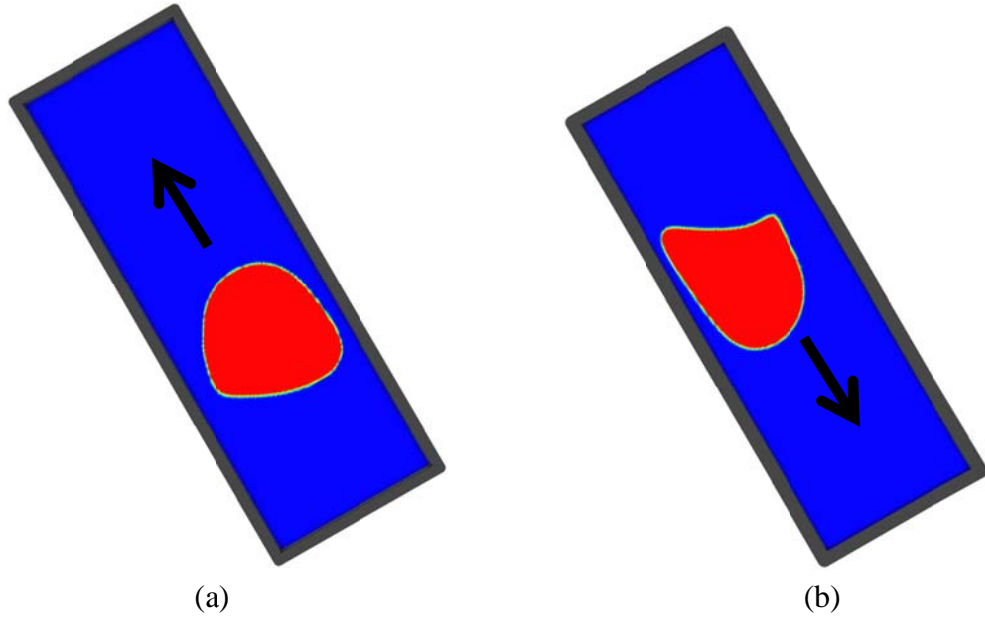


Figure 3.4: Effect of channel inclination ( $60^\circ$  inclination with horizontal) (a) on bubble (b) on drop

In this case efforts have been made to simulate the dynamics of 3D gaseous bubble in an inclined channel filled with high density fluid shown in Figure 3.4(a). Air ( $\rho_L = 1 \text{ kg/m}^3$ ) has been taken as gaseous bubble material and water ( $\rho_H = 1000 \text{ kg/m}^3$ ) has been taken as surrounding fluid. For the simulation of dynamics of bubble the diameter of the air bubble is taken as 80 mm and the channel dimension is taken as  $100 \text{ mm} \times 100 \text{ mm} \times 500 \text{ mm}$ . No slip boundary condition is applied at the solid vertical wall with bounce back condition at the adjacent lattices. Simulations have been made for three different inclinations of the channel ( $90^\circ$ ,  $60^\circ$  and  $30^\circ$ ) with horizontal.

Numerical simulation of water drop moving in stationary kerosene medium moving downward in inclined channel has also been done as shown in Figure 3.4(b). Channel size and boundary conditions are kept identical to that of the case of bubble dynamics.

# **Chapter 4**

## **Results and Discussion**

In present chapter obtained results of the problems described in Chapter 3 using the prescribed methodology (described in Chapter 2) have been discussed in detail. The consecutive explanations for each problem have also been discussed here. Various contours and graphs have also been depicted in respective sections with explanation. The results in details (case wise separately) are given below.

## 4.1 Single phase heat transfer in 2D square domain

A lattice Boltzmann method (LBM) is used to solve the energy equation in a test problem involving thermal conduction and then to investigate the suitability of LBM for a new class of problems.

### 4.1.1 High temperature at bottom plane only

Variation of temperature with high temperature at bottom plane and low temperature at remaining three planes in a 2D square domain has been studied. Figure 4.1 shows the temperature contour with temperature  $T_h = 100^{\circ}\text{C}$  at the bottom surface and  $T_c = 0^{\circ}\text{C}$  at the remaining three surfaces.

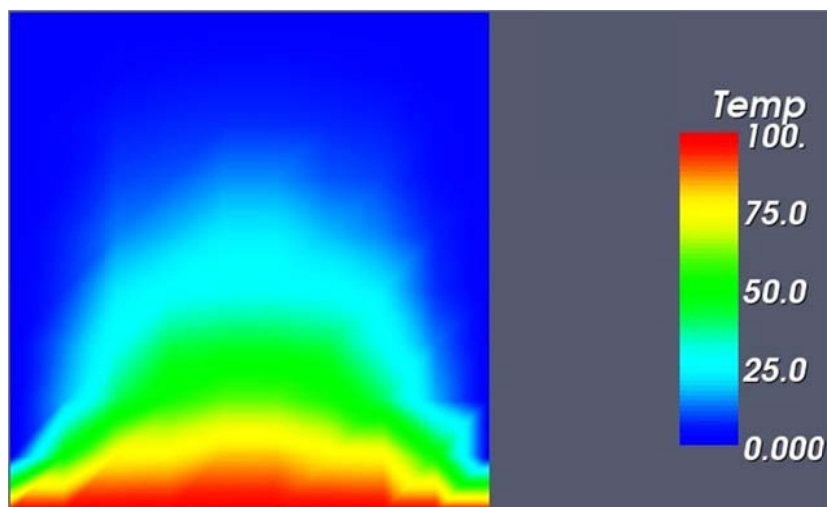


Figure 4.1: Temperature contour of 2D square domain with  $100^{\circ}\text{C}$  at bottom plane.

It is clear from the figure that temperature is decreasing from bottom plane to top plane. Figure 4.2 shows the plot between temperature and the distance from the bottom plane for mid plane of the square domain.

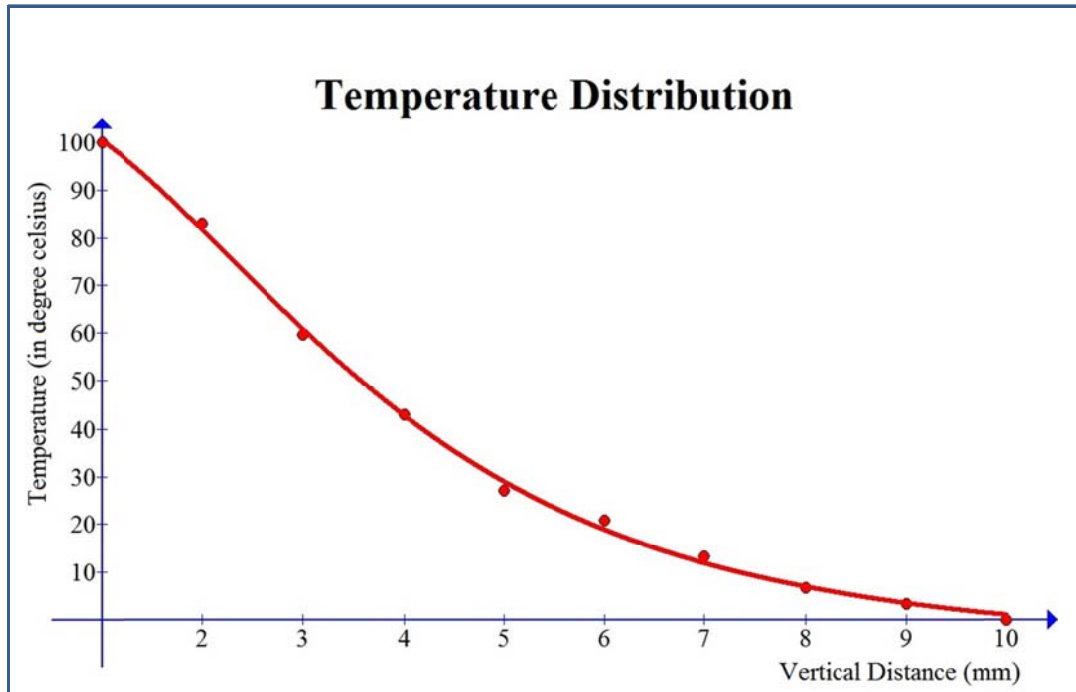


Figure 4.2: Temperature profile of vertical mid plane for 2D square domain with  $100^{\circ}\text{C}$  at bottom plane

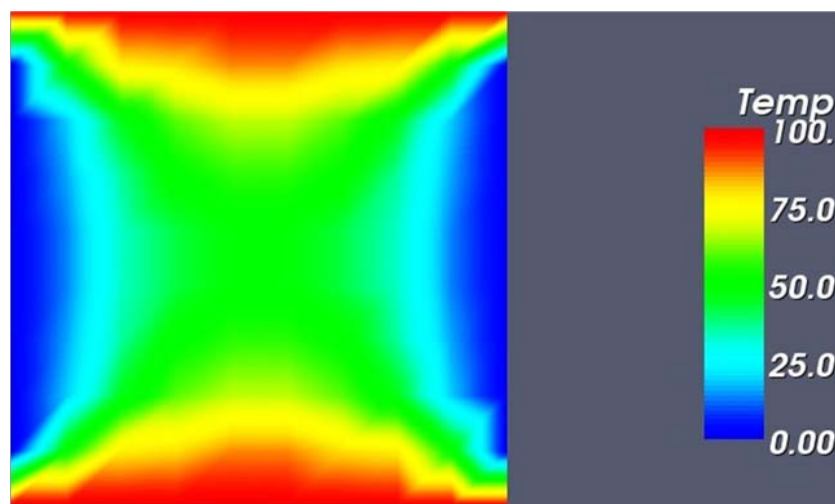


Figure 4.3: Temperature contour of 2D square domain for top and bottom plane at  $100^{\circ}\text{C}$  and remaining at  $0^{\circ}\text{C}$ .

### 4.1.2 High temperature at top and bottom plane

Figure 4.3 shows the temperature contour with temperature  $T_h = 100^{\circ}\text{C}$  at the bottom and top surface and  $T_c = 0^{\circ}\text{C}$  at the remaining two surfaces. It is clear from the figure that temperature is decreasing as somebody move from bottom plane to mid plane and again it increases as somebody move towards top plane. Figure 4.4 shows the plot between temperature and the distance from the bottom plane for mid plane of the square domain.

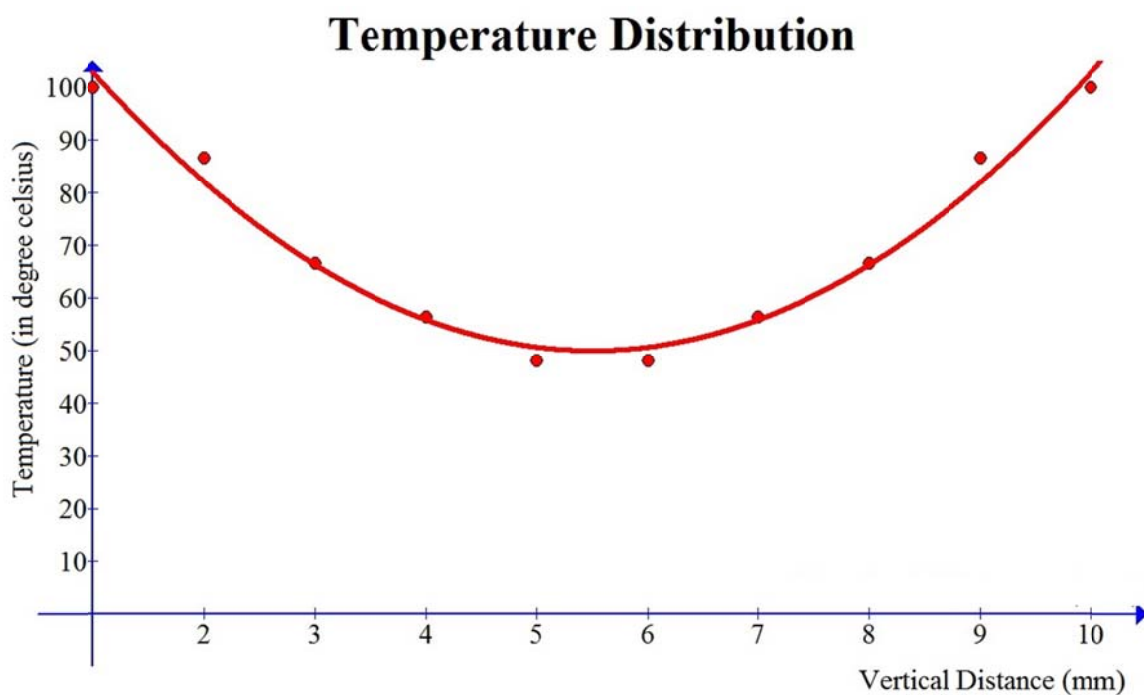


Figure 4.4: Temperature profiles for vertical mid plane for temperature of  $100^{\circ}\text{C}$  at top and bottom plane and remaining plane at  $0^{\circ}\text{C}$ .

### 4.2 Effect of fluid velocity on drop

The simulation has been started by considering a water drop at the top of the moving liquid (kerosene) column. Four different velocities 0m/s, 0.1m/s, 0.2m/s, 0.3m/s of kerosene matrix have been tried during the simulation. The phase contours obtained from the numerical simulations have been depicted in Figure 4.5a to 4.5c

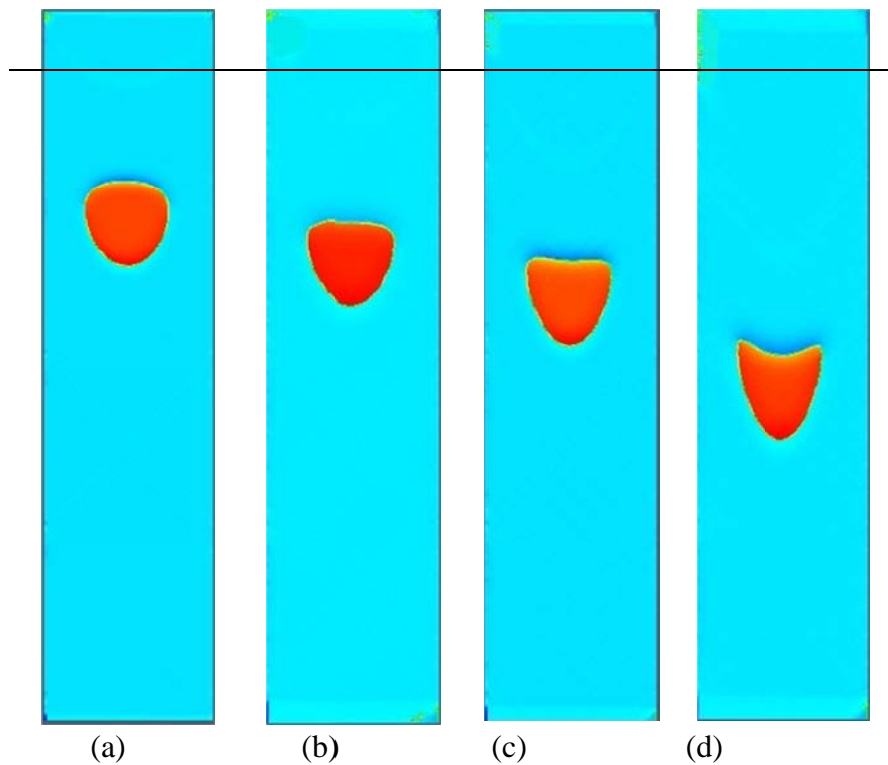


Figure 4.5: Effect of liquid velocity ( $V_L$ ) on the dynamics of drop: (a)  $V_L = 0\text{m/s}$  (b)  $V_L = 0.1\text{ m/s}$  (c)  $V_L = 0.2\text{ m/s}$  (d)  $V_L = 0.3\text{ m/s}$

It has been observed that for different magnitude of velocity, the circular drop moves. It is evident from the figures that circular drop remains symmetric as it moves downward direction. As the drop is bounded by the channel walls, the shape of the drop no longer remains circular. Moreover, the drops in all the situations turn into bullet like shape while moving downward. Bullet like shape of the drop is more pronounced as the velocity of surrounding fluid increases.

Effect of surrounding liquid velocity can be clearly identified from the respective position and shape of the drops at fixed time interval. Drop under the action of liquids having high velocity moves down faster compared to the situation where surrounding liquid velocity is low. The shape of the drop gets distorted due to the influence of its neighboring liquid velocity. As a result drop moving with velocity

of 0.3 m/s becomes more distorted as compared to the case where drop moving under liquid velocity of 0.1 m/s.

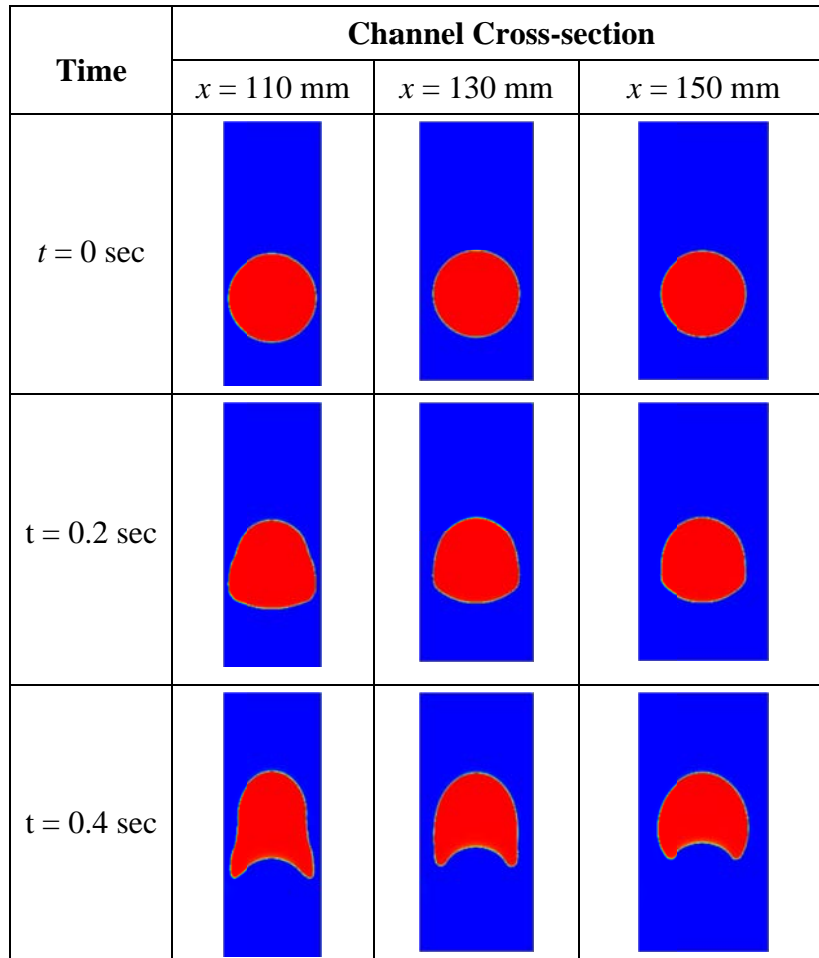


Figure 4.6: Effect of channel size on bubble shape at different time step

### 4.3 Effect of cross-section on bubble shape

In this case three different conduit configurations (110 mm × 500 mm, 130 mm × 500 mm and 150 mm × 500 mm) have been chosen for simulation. Bubble is placed in the water column symmetrically. Due to buoyant force bubble moves upward in the channel filled with water and its shape changes owing to no slip boundary condition applied at the wall. Phase contours at vertical plane have been reported in the Figure 4.6. Wall effect on the bubble shape is more pronounced for channels of smaller

cross-section. Shape of the bubble changes into a bullet like shape for smaller channel and symmetry across the axis of the conduit is maintained. For large conduit configuration shape of the bubble is more or less spherical.

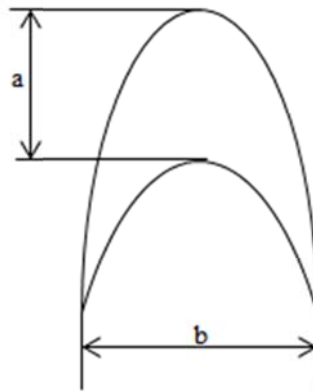


Figure 4.7: Deformed bubble at particular time step

Effect of channel size on the deformation of bubble can also be observed from the plots shown in the Figure 4.8. Plot between non dimensional parameter ‘c’ and time have been made for different conduit cross-section, where ‘c’ has been taken as ‘ $c = a/b$ ’ and ‘a’ and ‘b’ are shown in Figure 4.7. It is clear from Figure 4.8 that deformation of the bubble is more pronounced for smaller channel.

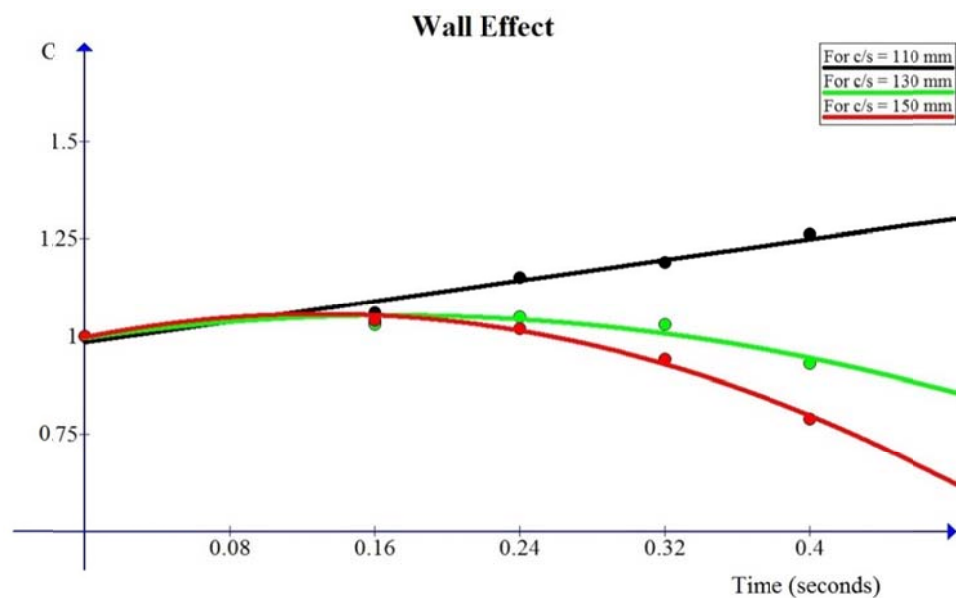


Figure 4.8: Effect of channel cross-section on the bubble shape

The effect of channel cross-section on the shape of the bubble decreases also with increase in channel size. Size of the channel also affects the velocity distribution within the gaseous phase of the bubble. As wall effect on the surface of the bubble is more pronounced in the case of smaller channel cross-section, velocity distribution along the surface of the bubble will be more. The velocity at the tail of the bubble with time instant has been plotted which is shown in Figure 4.9.

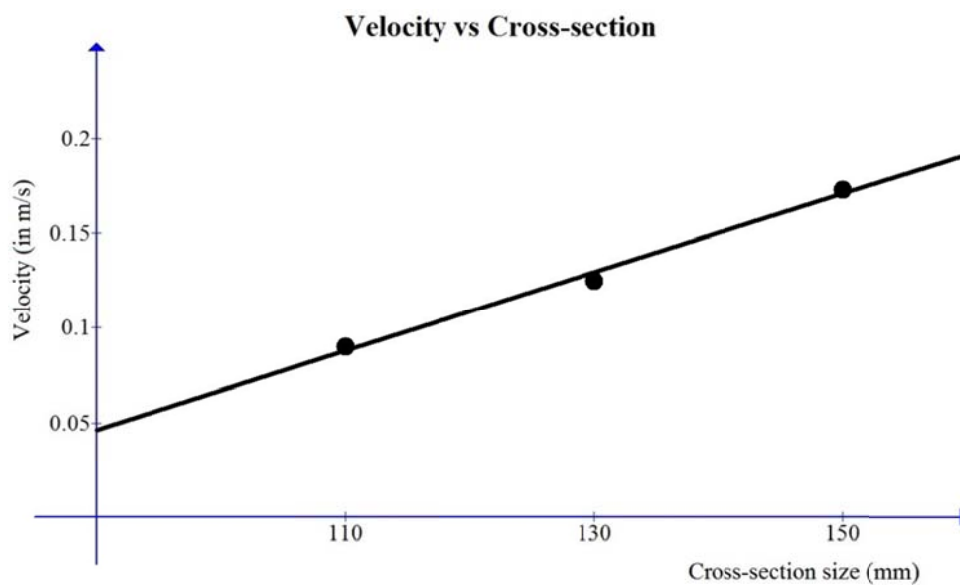


Figure 4.9: Effect of channel size on velocity of bubble

#### 4.4 Dynamics of bubble and drop in inclined channel

In this case a developed 3D Lattice Boltzmann Model has been used for simulation of dynamics of bubble and drop through the inclined channel.

##### 4.4.1. Effect of channel inclination on bubble

In this case simulations have been made for three different angle of inclinations of the channel position ( $90^\circ$ ,  $60^\circ$  and  $30^\circ$ ). The shapes and location of the bubbles for different inclination angle are depicted in Figure 4.10a to 4.1c. For a vertical

channel, it can be seen that the bubble becomes bullet shaped and remain symmetric across the channel axis. The symmetry is also clear from the sectional view as has been depicted in the Figure 4.10(a).

It has been observed that channel with  $60^\circ$  inclination angle, the bubble becomes asymmetric along the centerline of the channel. The trend of asymmetry increases with the inclination angle of the channel.

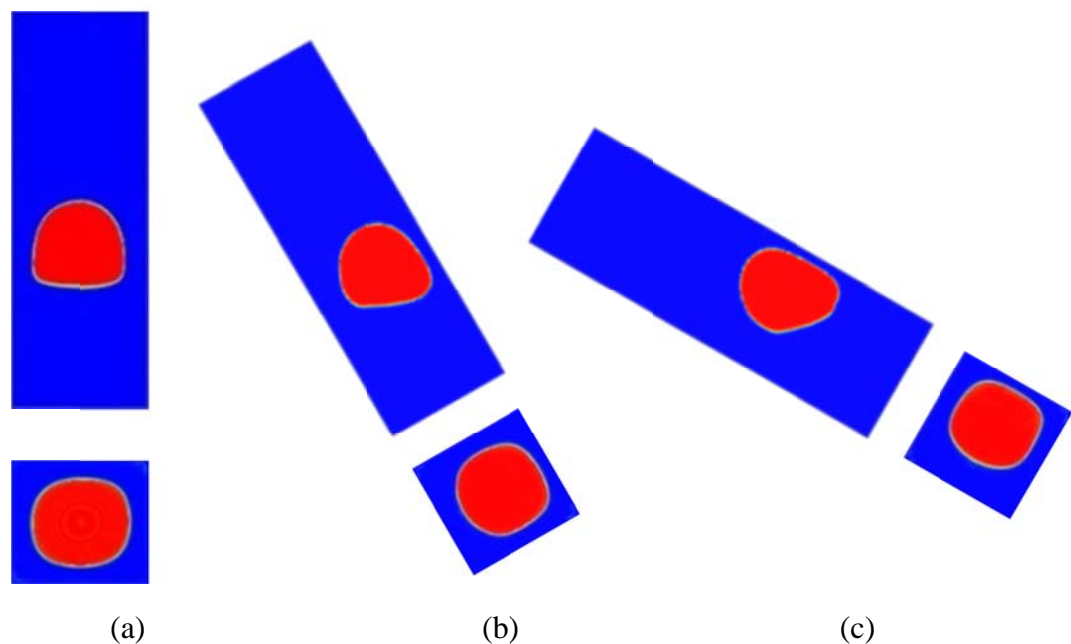


Figure 4.10: Effect of channel inclination on bubble asymmetry for (a)  $90^\circ$  inclination (b)  $60^\circ$  inclination (c)  $30^\circ$  inclination. For each figure lower part is showing the top view and upper part is showing the vertical sectional view.

#### 4.4.2. Effect of bubble volume

Bubble volume is obviously another parameter which influences the shape and location of the bubble in an inclined channel. Simulations have been made for different volumes of bubble ( $4.08 \times 10^{-4} \text{ m}^3$ ,  $2.68 \times 10^{-4} \text{ m}^3$ ,  $1.79 \times 10^{-4} \text{ m}^3$ ) passing through inclined channel. It has been observed that bubble with smaller volume

acquiring bullet shape very quickly. Because with the increase of bubble volume, the effect of wall becomes prominent.

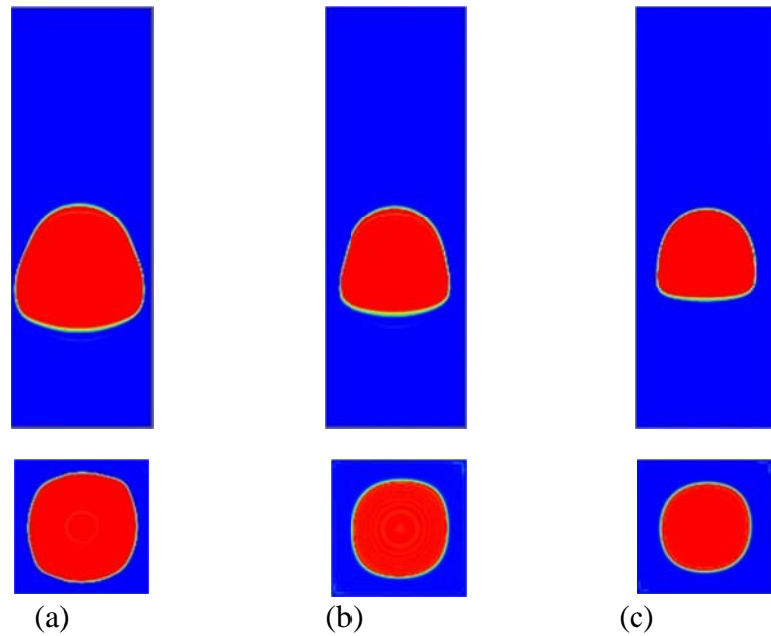


Figure 4.11: Effect of bubble volume on the shape of bubble in vertical channel with (a) volume =  $4.08 \times 10^{-4} \text{ m}^3$  (b) volume =  $2.68 \times 10^{-4} \text{ m}^3$  (c) volume =  $1.79 \times 10^{-4} \text{ m}^3$ . For each figure lower part is showing the top view and upper part is showing the vertical sectional view.

But the symmetricity of the bubble spoiled as the channel is inclined from its original vertical position. Asymmetry is observed for all three bubble volumes when the channel is inclined at  $60^\circ$  and  $30^\circ$  as shown in Figure 4.12 and 4.13 respectively. The effect of asymmetricity is higher for bubble with higher volume.

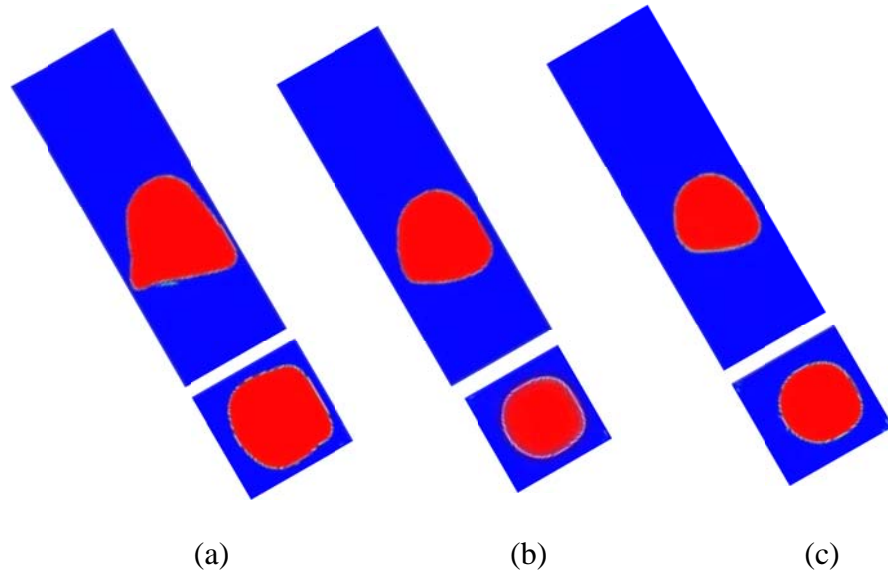


Figure 4.12: Effect of bubble volume on the shape of bubble in  $60^{\circ}$  inclined channel with (a) volume =  $4.08 \times 10^{-4} \text{ m}^3$  (b) volume =  $2.68 \times 10^{-4} \text{ m}^3$  (c) volume =  $1.79 \times 10^{-4} \text{ m}^3$ . For each figure lower part is showing the top view and upper part is showing the vertical sectional view.

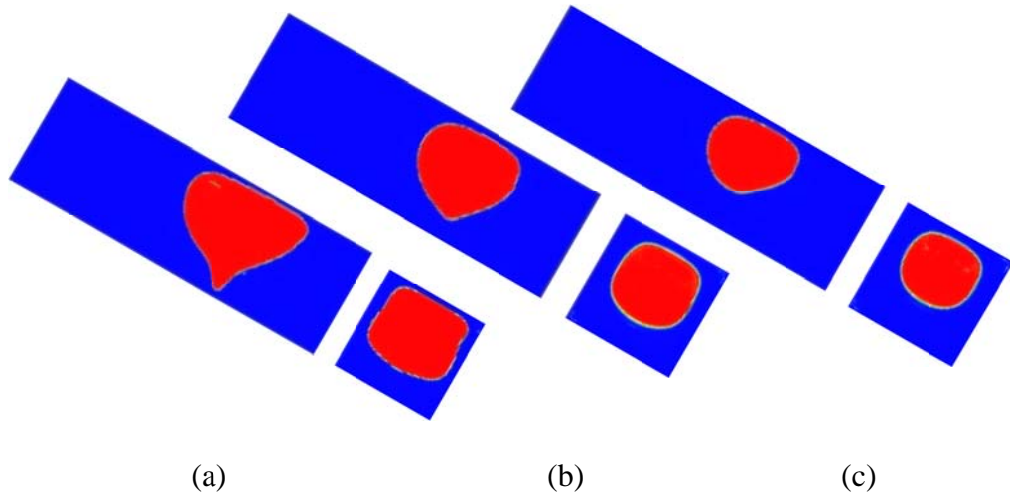


Figure 4.13: Effect of bubble volume on the shape of bubble in  $30^{\circ}$  inclined channel with (a) volume =  $4.08 \times 10^{-4} \text{ m}^3$  (b) volume =  $2.68 \times 10^{-4} \text{ m}^3$  (c) volume =  $1.79 \times 10^{-4} \text{ m}^3$ . For each figure lower part is showing the top view and upper part is showing the vertical sectional view.

#### 4.4.3 Effect of channel inclination on drop

In this section efforts have been made to simulate the dynamics of drop of liquid of higher density in the surrounding of lighter fluid medium in an inclined channel.

Water has been taken as drop in the surrounding of kerosene medium. Boundary conditions are kept identical as in section 4.4.1. Channel dimension has been taken as 100 mm×100 mm × 300 mm. The diameter of drop has been taken as 80mm. Simulation have been made for three different inclinations of the channel (90°, 60° and 30°) with the horizontal. The shapes and location of the drop for different inclinations are depicted in Figure 4.14a-c.

For a vertical tube it can be observed that the drop is bullet shaped and symmetric across the channel cross section. The symmetry is also clear from the sectional view as has been depicted in the vertical channel (Figure 4.14a). It has been observed that at 60° inclination with horizontal, the drop becomes asymmetric along the centerline of the channel.

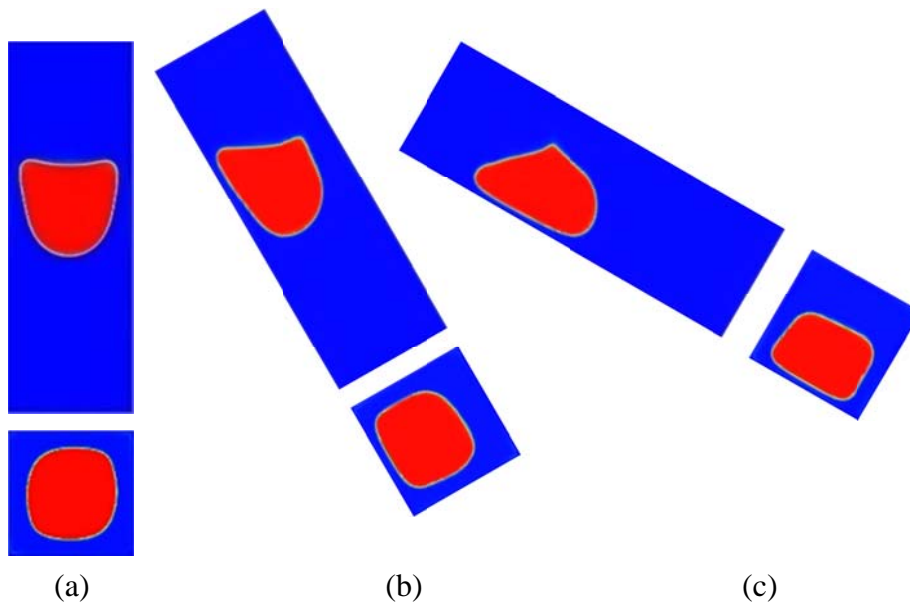


Figure 4.14: Effect of channel inclination on drop asymmetry for (a) 90° inclination (b) 60° inclination (c) 30° inclination.

This trend of asymmetry continues for higher inclinations of the channel. Asymmetry in the drop shapes increases as the inclination varies at 60° and 30° with horizontal. From the cross sectional view of all the figures, the asymmetry is quite clear.

#### 4.4.4 Effect of drop volume

Drop volume is another parameter which influences its shape and velocity during its downward motion. Simulations have been made for different volumes ( $4.08 \times 10^{-4} \text{ m}^3$ ,  $2.68 \times 10^{-4} \text{ m}^3$ ,  $1.79 \times 10^{-4} \text{ m}^3$ ) of the drop passing through inclined channel. It has been observed that drop retains symmetry while moving downward in vertical channel irrespective of volume. Figure 4.15a-c clearly shows the symmetric drop shape for three different volume of water drop moving through vertical kerosene column. Symmetric shape is also evident in their sectional view.

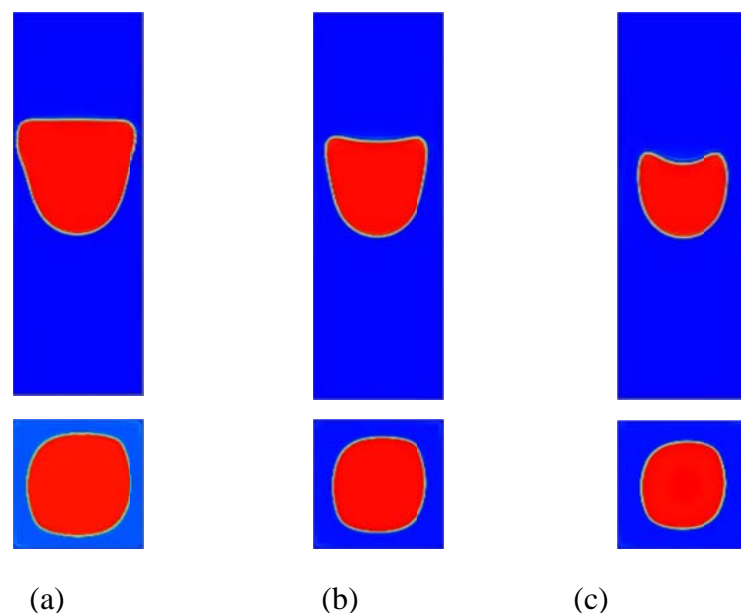


Figure 4.15: Effect of drop volume on the shape of drop in vertical channel with (a) volume =  $4.08 \times 10^{-4} \text{ m}^3$  (b) volume =  $2.68 \times 10^{-4} \text{ m}^3$  (c) volume =  $1.79 \times 10^{-4} \text{ m}^3$

But the symmetry of the drop shifts as the channel is inclined from its original vertical position. Asymmetry is observed for all three drop volumes when the channel is inclined at  $60^\circ$ . It is evident from the Figure 4.16a-c, and Figure 4.17a-c that drop becomes more asymmetric when its size decreases.

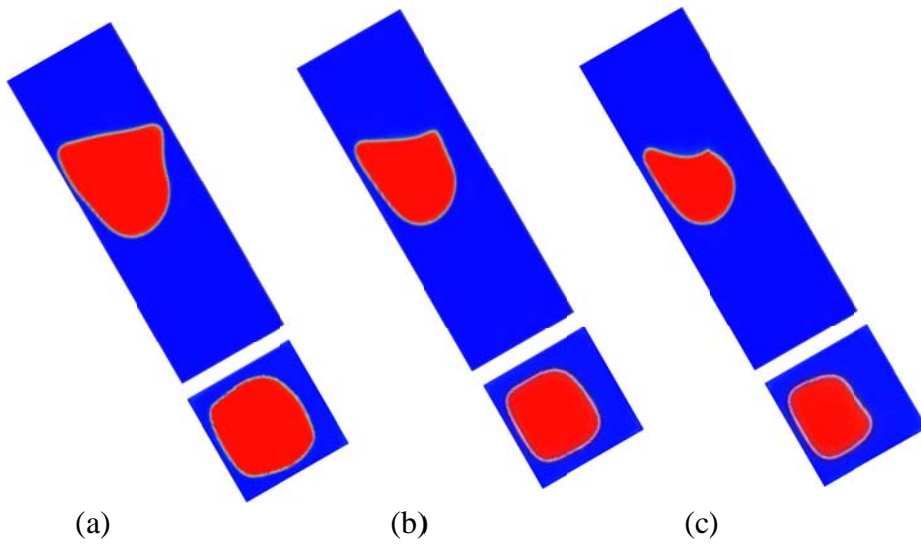


Figure 4.16: Effect of drop volume on the shape of drop in  $60^\circ$  inclined channel with (a) volume =  $4.08 \times 10^{-4} \text{ m}^3$  (b) volume =  $2.68 \times 10^{-4} \text{ m}^3$  (c) volume =  $1.79 \times 10^{-4} \text{ m}^3$

From the sectional views observations can be made that drop having volume  $1.79 \times 10^{-4} \text{ m}^3$  is more asymmetric as compared to the drop of volume  $2.68 \times 10^{-4} \text{ m}^3$ .

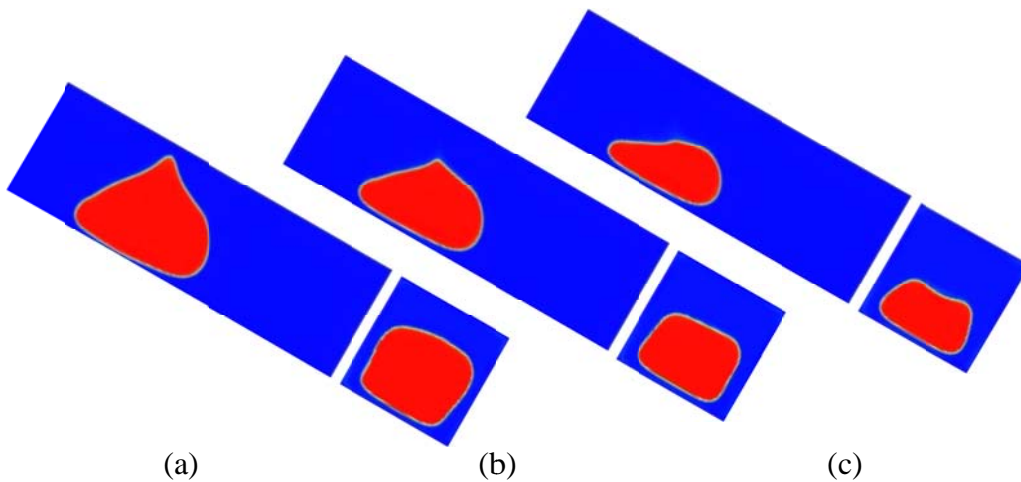


Figure 4.17: Effect of drop volume on the shape of drop in  $30^\circ$  inclined channel with (a) volume =  $4.08 \times 10^{-4} \text{ m}^3$  (b) volume =  $2.68 \times 10^{-4} \text{ m}^3$  (c) volume =  $1.79 \times 10^{-4} \text{ m}^3$

# **Chapter 5**

**Concluding Remarks**

**and**

**Future Scope**

In the present chapter the important findings from the overall study of the selected problems have been given. Concluding remarks and scope of the future work have also been discussed.

## **5.1 CONCLUDING REMARKS**

The important finding and concluding remarks about the present investigation are given below point wise.

### **5.1.1 Single phase heat transfer in 2D square domain**

- 2D heat transfer phenomena have been studied for different variations of boundary conduction using lattice Boltzmann model.
- Temperature contours has been shown for different boundary conditions.
- Temperature profiles are plotted for the vertical mid plane of the square domain.

### **5.1.2 Effect of fluid velocity on drop**

- The drop moves faster as the liquid velocity increases.
- Shape of drop is also influenced as the velocity of the surrounding liquid changes.
- The crater at the bottom position of the drop increases with the increase in velocity of liquid.

### **5.1.3 Effect of channel cross-section on bubble shape**

- Bubble becomes more distorted as channel size decreases.
- For smaller channel bubble becomes bullet like shape and for larger channel shape is more or less spherical.
- Velocity of bubble moving upward increases with increase of channel size.

### **5.1.3 Dynamics of a bubble and drop through inclined channel**

- Numerical model was efficient enough to capture the asymmetry in the shape of the drop or bubble under different inclinations of the channel.
- Simulations have been made for a wide range of drop or bubble volume.
- Asymmetry in the bubble or drop shapes increases as the inclination varies at 60° and 30° with horizontal.
- With the increase of bubble or drop volume the effect of wall becomes prominent which makes the bubble shape similar to a bullet.
- Bubble or drop becomes more asymmetric with the axis of channel when its volume decreases.

## **5.2 Future scope**

Based on the work done in this session following topics can be done in next session:

- Proper combinations of thermal and two phase lattice Boltzmann method can simulate complicated bubble column reactor.
- 3D lattice Boltzmann model can be used for complicated channel geometry like sudden contraction and expansion or sharp return bend.
- Heat transfer model can be extrapolated for different complicated boundary conditions and inside intrusions.



# References

- Bhaga, D., Weber, M.E., 1981. Bubbles in viscous liquids: shapes, wakes and velocities. *J. Fluid Mech.* 105 61–85.
- Bhatnagar, P., Gross, E.P., Krook, M.K., 1954. A model for collision processes in gases. *Phys. Rev.* 94.
- Bozzano, G., Dente M., 2001. Shape and terminal velocity of single bubble motion: a novel approach. *J. Computers and Chemical Engineering*, 25, pp. 571-576.
- Bretherton, F.P., 1961. The motion of long bubbles in tubes, *J. Fluid Mech.* 10, 166–188.
- Cahn, J.W., Hilliard, J.E., 1958. Free energy of a non-uniform system. I. Interfacial energy, *J. Chem. Phys.* 28 (2) 258–267.
- Chen, S., Doolen G., 1998. Lattice Boltzmann method for fluid flows. *Annu. Rev. Fluid Mech.* 30 329–364.
- Frisch, U., Hasslacher, B., Pomeau, Y., 1986. Lattice-Gas Automata for the Navier-Stokes Equation, *Phys. Rev. Lett.* 56, 1505–1508.
- He, X., Chen, S., Zhang R., 1999. A lattice Boltzmann scheme for incompressible multiphase flow and its application in simulation of Rayleigh–Taylor instability. *J. Comput. Phys.*, 152, (2), pp. 642-663.
- Inamuro, T., Ogata, T., Tajima, S., Konishi, N., 2004. A lattice Boltzmann method for incompressible two-phase flows with large density differences, *J. Comput. Phys.* 198 628–644.
- Kataoka, Y., Suzuki, H., Murase, M., 1987. Drift-flux parameters for upward gas flow in stagnant liquid. *J. Nucl. Sci. Technol.* 24, 580–586.

- Lee, T., Lin, C.-L., 2005. A stable discretization of the lattice Boltzmann equation for simulation of incompressible two-phase flows at high density ratio, *J. Comput. Phys.* 206 16–47.
- Lu, X., Prosperetti, A., 2006. Axial stability of Taylor bubbles. *J. Fluid Mech.* 568:173-192.
- Mandal, Tapas K., Das, Gargi., Das, Prasanta K., 2008. Motion of Taylor Bubbles and Taylor Drops in Liquid-Liquid Systems. *J. Ind. Eng. Chem. Res.*, 47, pp. 7048-7057.
- Polonsky, S., Shemer, L., Barnea, D., 1999. Relation between the Taylor bubble motion and the velocity field ahead of it. *Int. J. Multiphase Flow* 25, 957–975.
- Rothman, D.H., Keller, J.M., 1988. Immiscible cellular automaton fluid. *J. Stat. Phys.* 52:1119-1127.
- Shan, X., Chen, H., 1993. Lattice Boltzmann model for simulating flows with multiple phases and components, *Phys. Rev. E* 47 (3) 1815–1819.
- Swift, M.R., Osborn, W.R., Yeomans, J.M., 1996. Lattice Boltzmann simulation of liquid–gas and binary fluid systems, *Phys. Rev. E* 54 5041–5052.
- Takada, N., Misawa, M., Tomiyama, A., Hosokawa, S., 2001. Simulation of bubble motion under gravity by Lattice Boltzmann Method, *J. Nucl. Sci. Technol.* 38 (5) 330–341.
- Tudose, E.T. and Kawaji, M., 1999. Experimental investigation of Taylor bubble acceleration mechanism in slug flow. *Chem. Eng. Sci.* 54, 5671–5775.
- Tung, K.W. and Parlange, J.Y., 1976. Note on the motion of long bubbles in closed tube influence of surface tension, *Acta Mechanica* 24, 313–317..

Zheng, H. W., Shu, C., Chew, Y. T., 2006. A lattice Boltzmann for multiphase flows with large density ratio. *J. Comput. Phys.*, 218 pp. 353-371. *ogenics* 39, 803–809.

Zukoski, E.E., 1966. Influence of viscosity, surface tension and inclination angle on motion of long bubbles in closed tubes. *Journal of Fluid Mechanics* 25, 821–837.